Electronic Supplementary Material (ESI) for ChemComm.

Supporting Information

Hard-Soft Chemistry Guides the Adaptable Charge Transport in Lysine-doped Heptapeptide Junctions

*Ying Li, Xiaobing Li, Pan Qi, and Cunlan Guo**

College of Chemistry and Molecular Sciences, Wuhan University, Wuhan 430072, P. R. China

Email: cunlanguo@whu.edu.cn

1. Experiments and characterizations

1.1 Chemical reagents

Deionized water (18.2 MΩ·cm) was purified by using PURELAB Ultra from ELGA LabWater company. 36.0-38.0% hydrochloric acid (HCl) and 99.7% ethanol were purchased from Sinopharm Chemical Reagent Co., Ltd. Potassium hydroxide (KOH) and N, N-diisopropylethylamine (DIEA) were purchased from Aladdin. Trifluoroacetic acid (TFA), heptafluorobutyric acid (HFBA), triethylamine (TEA), and Eutectic gallium-indium (EGaIn) (purity ≥ 99.99%) were purchased from Sigma-Aldrich. All peptides with an MPA linker at the N terminus were purchased from GL Biochem. with purity > 95% (HPLC) and were stored at -20 °C. The optical adhesive was purchased from Norland (NOA 61). All chemical reagents were used as obtained except statements.

1.2 Preparation of gold substrate and peptide self-assembled monolayers (SAMs)

We prepared the ultraflat Au substrates (Au^{TS}) by the template stripping method.[1, 2] The Si wafer was cleaned by sonication in deionized water, acetone, and isopropyl alcohol for 3 minutes respectively, and dried by N_2 immediately. The cleaned Si wafer was treated by plasma for 3 minutes under 1:1 Ar and O_2, etched by 2% HF for 2 minutes, rinsed thoroughly with deionized water, and dried in a stream of N_2. After one repetition, the Si wafer was treated by plasma for 10 minutes under O_2. Next, we deposited gold on the Si wafer to form a ~100 nm gold film by a thermal evaporator. The cleaned glass slides (~1 × 1 cm^2) were placed on the gold film using optical adhesive. Then, the adhesive was cured for 4 hours by UV light. The fresh Au substrates were stripped from the Si wafer and immediately used for the following preparation of peptide SAMs.

Each type of peptides was dissolved in deionized water (0.01-0.02 mM) and the Au substrates were incubated in the newly prepared peptide solution at room temperature under a N_2 atmosphere without light for ~9 hours. The peptide SAMs under neutral condition were obtained after thoroughly rinsing with deionized water to remove peptides and drying in a stream of N_2. To investigate the effects of counterions on the

charge transport, the thoroughly rinsed peptide SAMs were immersed in acid or alkali solutions for 1 hour, and then rinsed with ethanol and dried in a stream of N_2. The concentrations of HCl and KOH were both 0.1 M, while those of organic acids and alkalis were all 1 M (TFA (pKa = 0.3), HFBA (pKa = 0.37), TEA (pKa = 10.78), and DIEA (pKa = 10.98)).

1.3 Thickness measurement

A J.A. Woollam M-2000® spectroscopic ellipsometer was used to characterize the peptide SAM thickness. The data were collected at incident angles of 60°, 70°, and 75° with an assumed refractive index of 1.50 for the organic SAM.[3, 4] The thickness was calculated via a two-layer model. One layer is the bottom Au layer, whose optical constant was determined by freshly prepared bare Au substrate; the other layer is the peptide SAM. The thickness of each peptide SAM was estimated by using the Cauchy model.

1.4 Topography by atomic force microscopy (AFM)

A Park NX10 AFM was used to characterize the surface topography of the bare gold substrate and the peptide SAMs. An aluminum-coated cantilever tip (HQ: XCS11/Al tip from MikroMasch, spring constant ~2 N/m, resonance frequency ~80 kHz, sensitivity ~45 V/μm) was used to obtain 1 × 1 μm^2 AFM images in tapping mode at a scan rate of 1 Hz.

1.5 Polarization modulation-infrared reflection-absorption spectroscopy (PM-IRRAS)

A Bruker INVENIO R Fourier transform infrared spectrometer (FT-IR) was used to perform IR spectroscopic characterization. The p- and s-polarized radiation were generated by passing the IR beam through a photoelastic modulator. The reflected polarized light by sample was directed into a liquid nitrogen cooled mercury cadmium telluride (MCT) detector at an incidence angle of 85°. To obtain the highest ratio of signal to noise around the amide vibration modes, the half-wave retardation frequency was set. 2000 interferograms with a band resolution of 4 cm^{-1} were collected and averaged as the final spectra.

1.6 J-V curves by electrical measurements

A Keithley 6430 Sub-Femtoamp Source-Meter was used to measure the J-V curves of peptide SAMs with a step value of 10 mV. A conical-tip EGaIn was applied as the top electrode to contact the SAM gently and the Au substrate served as the bottom electrode to form the Au^{TS}-peptides//GaO_x/EGaIn junctions. The shape of contact area was approximate a circle and the area was estimated by $¼\pi D^2$.[5] More than 20 junctions were formed for each peptide SAM and 15-17 J-V scans between -0.5 V and +0.5 V were measured for each junction. Finally, we collected more than ~280 J-V curves for each type of peptide SAMs. The log|J| value at -0.5 V for each peptide SAM junction was determined by statistics.

1.7 Ultraviolet photoemission spectroscopy (UPS)

A Thermo ESCALAB 250Xi ultraviolet photoelectron spectrometer was used to characterize the electronic structures of each type of peptide SAMs on the Au substrate under ultra-high vacuum (< 10^{-8} torr). UPS was obtained with a He-gas discharge lamp (He-Iα at 21.22 eV) and a Au standard sample was used for calibration. The energy resolution was 0.03 eV. In our work, we aligned the Fermi levels between the peptide/Au and bare Au reference. Taken the UPS data of K-1 SAM as an example, we illustrated the procedure of obtaining W_F and ΔE (Fig. S16). W_F was obtained from the intersection of linear extrapolation of the secondary electron cutoff spectrum and linear extrapolation of the baseline. We obtained ΔE at a logarithmic intensity scale due to the unclear signal of peptides on a linear scale. ΔE at low binding energy was obtained by extrapolating the signal edge to the background signal.

2. The calculation of skewness and kurtosis

We used the mean (μ) and the standard deviation (σ) of x (log|J|) from log|J| histogram to calculate skewness and kurtosis. All calculations were completed by Matlab. The skewness is defined as eq 1 and the kurtosis is defined as eq 2.[6, 7] Here, the $E(X)$ is the expectation of X.

$$S = \frac{E(x-\mu)^3}{\sigma^3} \quad \text{(eq 1)}$$

$$K = \frac{E(x-\mu)^4}{\sigma^4} \quad \text{(eq 2)}$$

3. Angle-resolved X-ray photoelectron spectroscopy (AR-XPS)

An AR-XPS (Analytical Ltd. AXIS ULTRA) was used to measure the surface coverage of peptide SAMs on the Au substrate. AR-XPS measurements were performed by using Al K_a (1486.6 eV) with a base pressure of 1×10^{-10} mbar. The location of the analyzer was fixed and the angle between it and the X-ray remained at 43º. AR-XPS detected electrons emitted from different angles by rotating the sample holder. We used the signal intensity of S *2p* spectra collected at take-off angle (θ) of 90º and 47º as well as incident angle (γ) of 47º and 90º to estimate the surface coverage of peptide SAMs. The take-off angle (θ) is defined as the angle between the axis of the analyzer and the Au substrate. The incident angle (γ) is defined as the angle between the beam incidence and the Au substrate.

The details on the surface coverage calculation are as follows.

First, d_2, the distance from the S atom to vacuum, was calculated by eq 3: [8, 9]

$$\frac{I_\theta\,(d,\ 90°)}{I_\theta\,(d,\ 47°)} = \frac{(1-e^{-\frac{d_1}{\lambda \sin 90°}})e^{-\frac{d_2}{\lambda \sin 90°}}}{(1-e^{-\frac{d_1}{\lambda \sin 47°}})e^{-\frac{d_2}{\lambda \sin 47°}}} \quad \text{(eq 3)}$$

d_1 (1.5 Å) is the distance between the S atom center and S-C bond center. The effective intensity (I_θ) in eq 1 was obtained by correcting the intensity of the spectrum (I) using eq 4:

$$I_\theta = I\,cos\,(90° - \gamma) \quad \text{(eq 4)}$$

λ is the inelastic free mean path and was calculated based on the equation derived from alkanethiol SAMs, [10] as shown in eq 5:

$$\lambda = 0.3E^{0.64} \quad \text{(eq 5)}$$

where E is the kinetic energy of a photoelectron. Here, λ is about 30 Å when E is at ~ 1325 eV.

Second, the S signal before attenuation (I_0) was calculated by eq 6:

$$I_0 = \frac{I_\theta}{e^{-\frac{d_2}{\lambda \sin\theta}}} \quad \text{(eq 6)}$$

Finally, we used 1-decanethiol SAM as the reference, the surface coverage of peptide SAMs can be calculated by eq 7:

$$\frac{I_0\,(ref)}{I_0\,(peptide)} = \frac{coverage\,(ref)}{coverage\,(peptide)} \quad \text{(eq 7)}$$

$I_{0(peptide)}$ and $I_{0(ref)}$ were calculated by the same way, and the surface coverage of reference, 1-decanethiol SAM, was 7.9×10^{-10} mol/cm^2.[11]

The surface coverage of peptide SAMs on the Au substrate is 3.45×10^{-10}, 6.93×10^{-10}, and 11.66×10^{-10} mol/cm^2 for K-1, K-4, and K-7 SAMs, respectively. The AR-XPS data were included in another work[12].

4. Landauer formula

To evaluate the J-V behaviors through peptide SAMs under diverse conditions, we fitted the experimental J -V data ranging from -0.5 to +0.5 V based on Landauer formula (eq. 3).[13]

$$I \cong N\frac{2e}{h}\Gamma_g{}^2\frac{eV}{(\varepsilon_0 + \alpha eV)^2 - \left(\frac{eV}{2}\right)^2} \quad \text{(eq. 8)}$$

where e is the charge of electron, h is the Plank's constant, α is asymmetric factor, and N is the effective number of molecules participating in the current. The values of N are 4.08×10^9, 8.19×10^9, and 1.38×10^{10} for K-1, K-4, and K-7, respectively, from our unpublished data, which were calculated from the coverage of peptide molecules by XPS and the contact area of the top electrode (GaO_x/EGaIn) on the peptide SAMs.

We mainly checked two parameters to estimate the conductance results: (i) the molecules-electrodes energy barrier height (ε_0) at zero bias, which is the energy difference between the closest orbital energy of peptide SAMs (HOMO or LUMO) and the Fermi level of electrode; and (ii) the energy level coupling between peptide SAMs and electrode (Γ_g), $\Gamma_g \equiv \sqrt{\Gamma_N \Gamma_C}$, where Γ_N and Γ_C are the energy level coupling at N-terminus and C-terminus of peptides with electrode interfaces.

5. Effect of neutral molecules on charge transport of peptide SAMs

To evaluate the effect of neutral molecules with similar size, we selected two ionic compounds, LiCl and KCl, to separately study their effects on the charge transport of K-1 and K-7 SAMs. The LiCl and KCl treated K-1 and K-7 SAMs were first characterized by XPS, AFM, ellipsometry measurements, and PM-IRRAS. The XPS measurements verified the presence of LiCl or KCl in K-1 and K-7 SAMs (Fig. 20). After LiCl or KCl treatments, the thickness of the peptide SAMs did not increase significantly and was similar to that of the neutral SAMs (Table S3), indicating no over-adsorbed ions on the peptide SAMs. The peptide SAMs were densely packed according to AFM images (Fig. 21). Compared with the peptide SAMs before treatment, the amide bands and amide I/II ratios of LiCl- or KCl-treated SAMs were almost unchanged (Fig. 22 and Table S4), indicating that the LiCl/KCl did not significantly change the conformation of peptides and the interactions between peptide SAMs and LiCl or KCl were weak.

The charge transport of the treated peptide SAMs was then studied. The log|J| distribution histograms of peptide SAMs were shown in Figs. 23-24 and the J-V curves were shown in Fig. 25. The effect of LiCl and KCl on the charge transport of peptide SAMs were summarized in the ΔJ/J plots (Fig. 26). LiCl and KCl can be compared with each other for the same-sized anions and different-sized cations (Li^+ < K^+). The effects of KCl and LiCl on the charge transport of peptide SAMs are very similar to each other and are all smaller than the ones treated by acid or base.

Figures and Tables

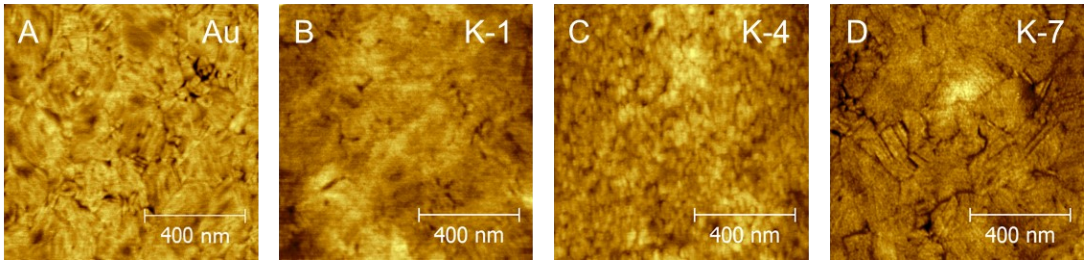

Fig. S1 Surface topographies of peptide SAMs measured by AFM images. (A) Bare Au substrate, (B) K-1, (C) K-4, and (D) K-7 peptide SAMs under neutral condition.

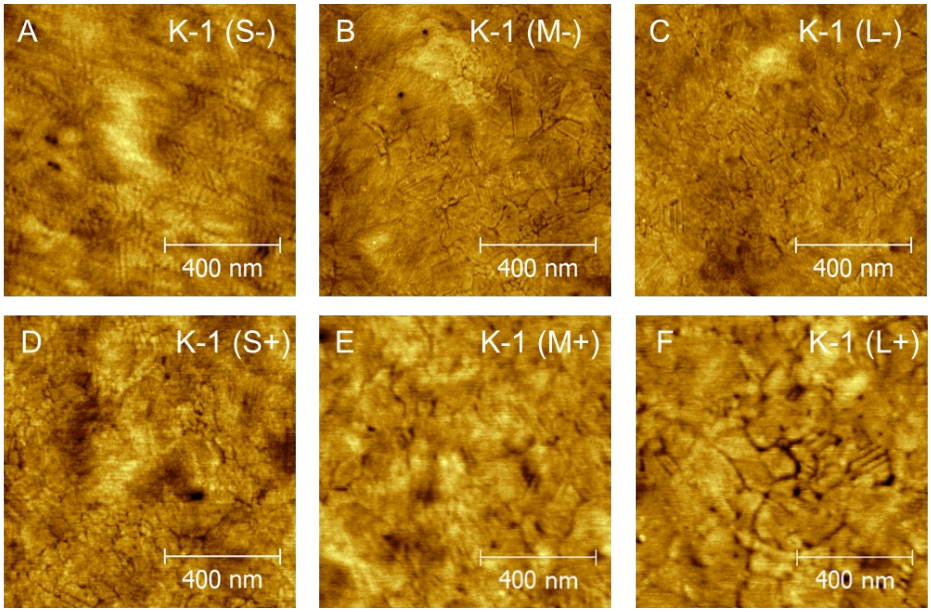

Fig. S2 AFM images of K-1 peptide SAMs under different conditions. (A-C) Under protonated conditions of HCl (S-), TFA (M-), and HFBA (L-). (D-F) Under deprotonated conditions of KOH (S+), TEA (M+), and DIEA (L+). The symbol of - and + represent the conjugate alkalis of acids and conjugate acids of alkalis, respectively, while the S, M, and L indicate the small (HCl, KOH), medium (TFA, TEA), and large size (HFBA, DIEA) of counterions, respectively.

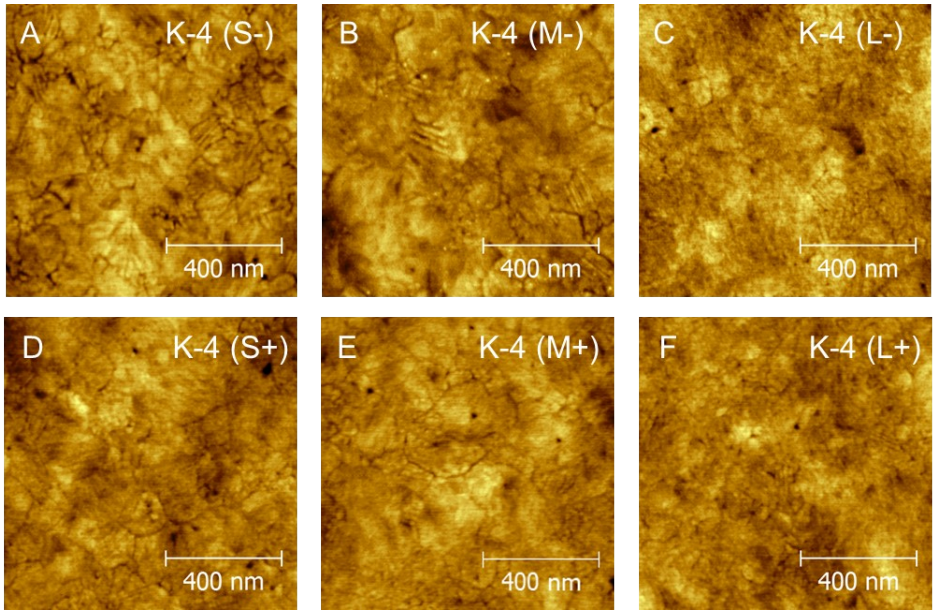

Fig. S3 AFM images of K-4 peptide SAMs under different conditions. (A-C) Under protonated conditions of HCl (S-), TFA (M-), and HFBA (L-). (D-F) Under deprotonated conditions of KOH (S+), TEA (M+), and DIEA (L+). The symbol of - and + represent the conjugate alkalis of acids and conjugate acids of alkalis, respectively, while the S, M, and L indicate the small (HCl, KOH), medium (TFA, TEA), and large size (HFBA, DIEA) of counterions, respectively.

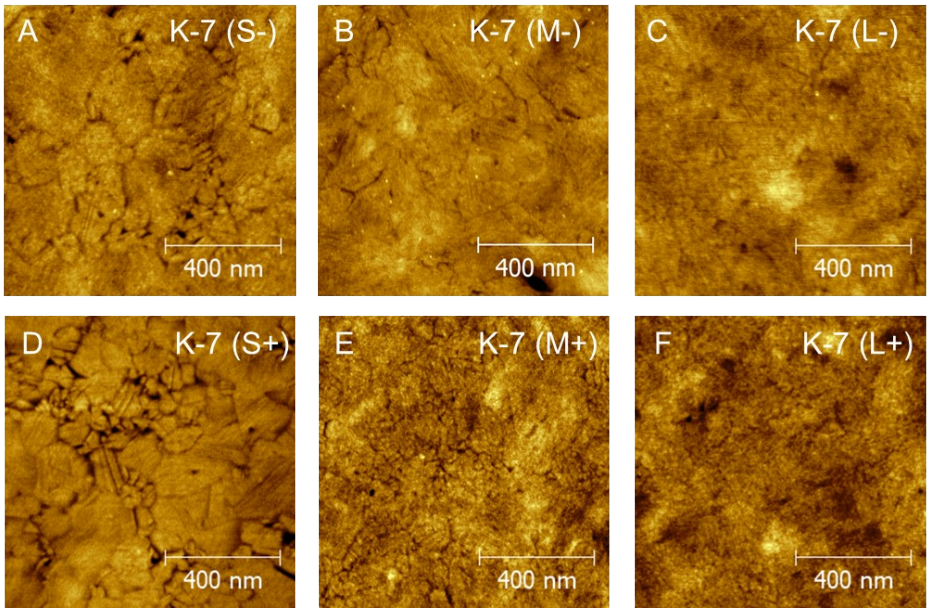

Fig. S4 AFM images of K-7 peptide SAMs under different conditions. (A-C) Under protonated conditions of HCl (S-), TFA (M-), and HFBA (L-). (D-F) Under deprotonated conditions of KOH (S+), TEA (M+), and DIEA (L+). The symbol of - and + represent the conjugate alkalis of acids and conjugate acids of alkalis, respectively, while the S, M, and L indicate the small (HCl, KOH), medium (TFA, TEA), and large size (HFBA, DIEA) of counterions, respectively.

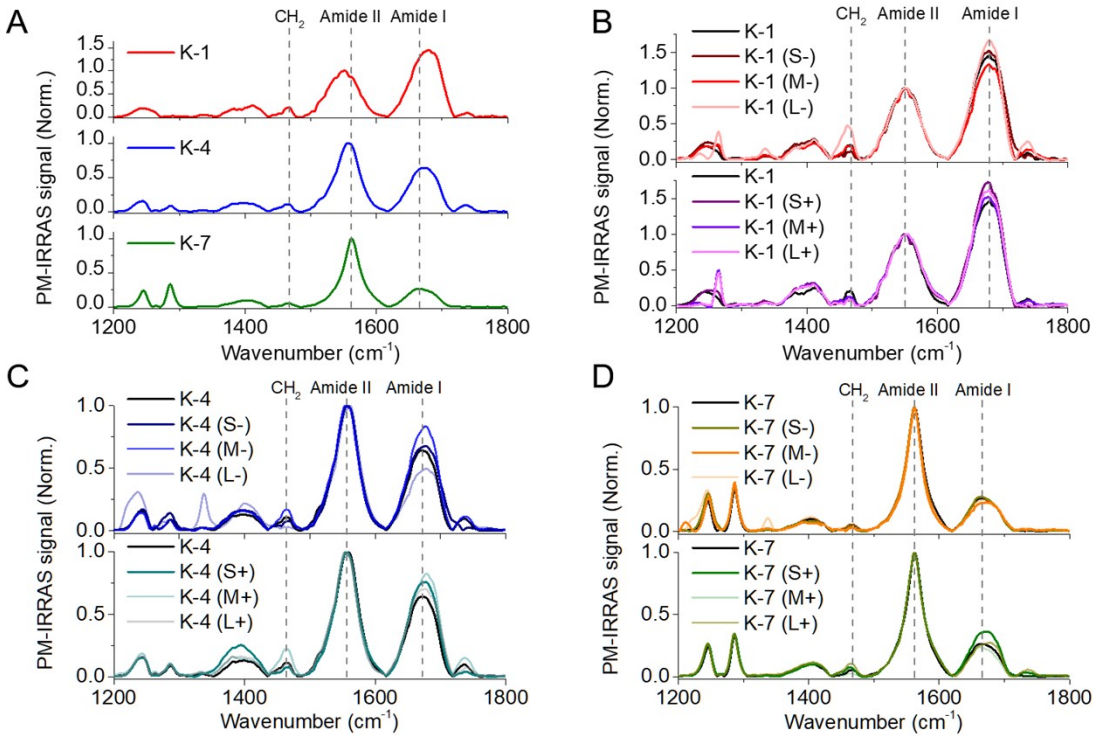

Fig. S5 Normalized PM-IRRAS spectra of the peptide SAMs with 4 cm^{-1} band resolution in the range of 1200-1800 cm^{-1}. (A) Peptide SAMs under neutral condition. (B) K-1, (C) K-4 and (D) K-7 under different conditions. In panels B-D, the upper and lower portions are the IR curves under protonated and deprotonated conditions, respectively. The black curves show the IR curves under neutral condition in panels B-D for comparison.

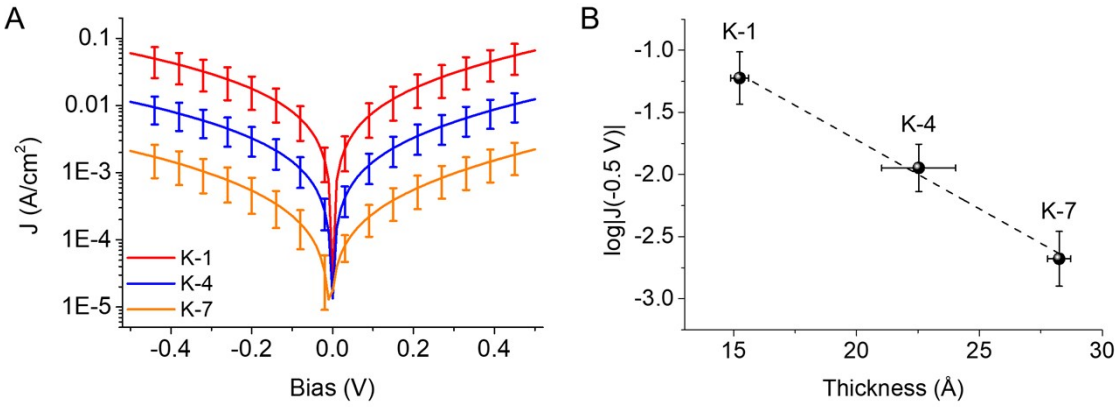

Fig. S6 Current density data for K-1, K-4, and K-7 peptide junctions under neutral conditions. (A) Semilog plots of J-V for K-1, K-4, and K-7 peptide junctions under neutral conditions. (B) log|J| at -0.5 V varies with thickness for K-1, K-4, and K-7 peptide SAMs.

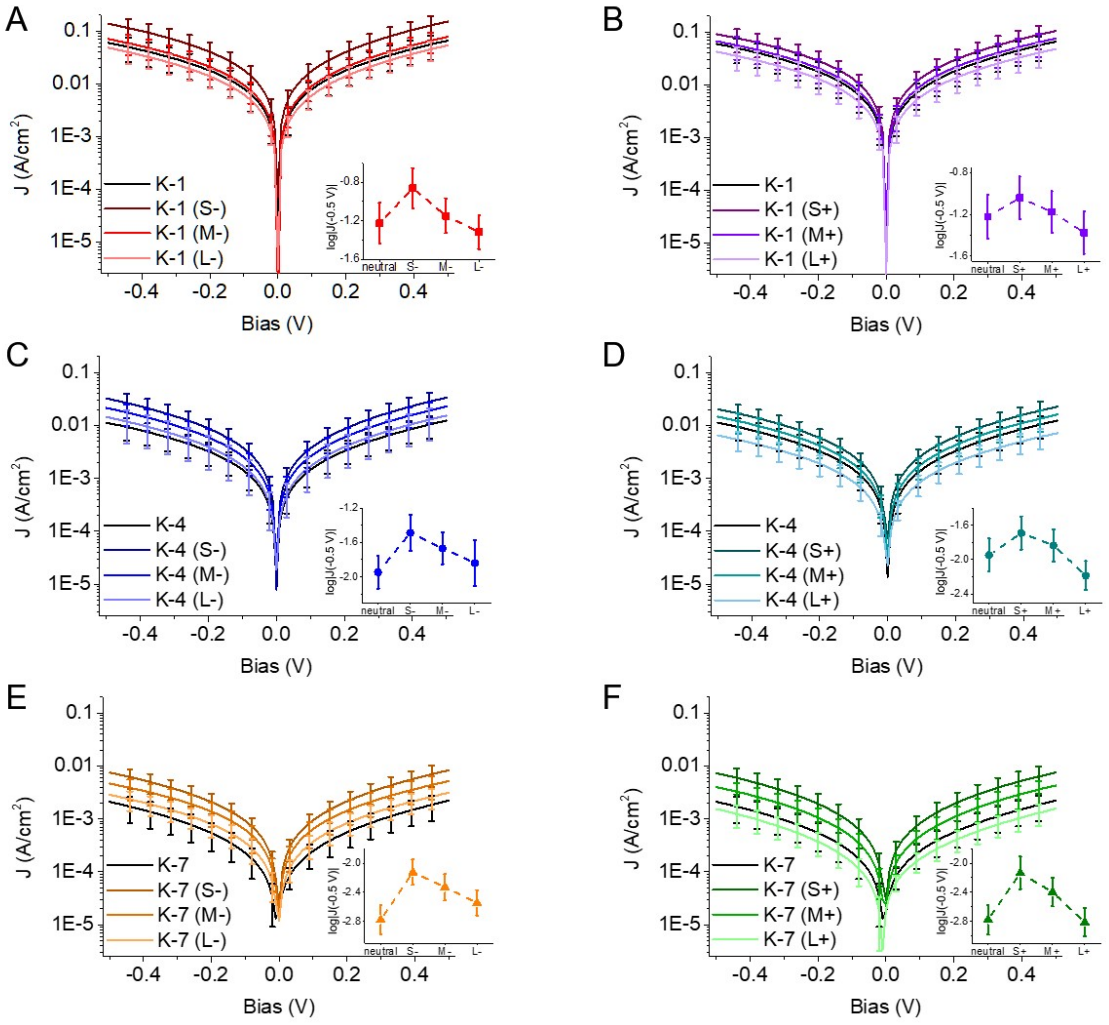

Fig. S7 Semilog plots of J-V for K-1, K-4, and K-7 peptide junctions under different conditions. (A), (C), and (E) K-1, K-4, and K-7 peptide SAMs under protonated conditions, respectively. (B), (D) and (F) K-1, K-4, and K-7 peptide SAMs under deprotonated conditions, respectively. The black curves show the J-V plots under neutral condition in all panels for comparison. Inset: the variation trends of log|J| at -0.5 V under different conditions.

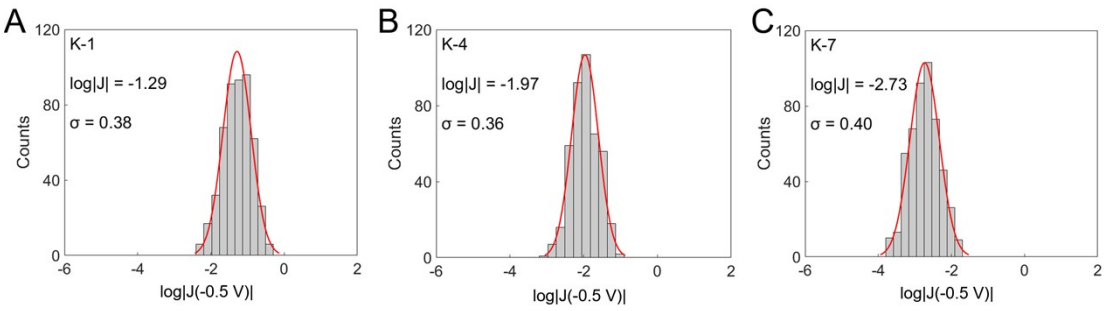

Fig. S8 log|J| distribution histograms of peptide SAM junctions at -0.5 V under neutral condition: (A) K-1. (B) K-4. (C) K-7. The red curves represent the Gaussian fits to these histograms. All J-V measurements were performed at room temperature.

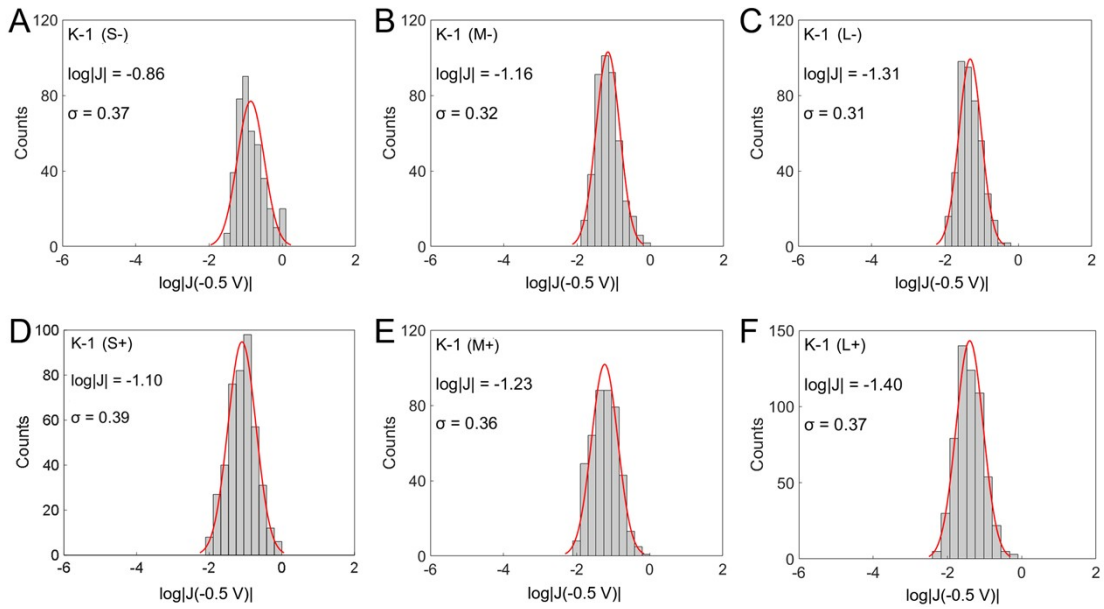

Fig. S9 log|J| distribution histograms of K-1 peptide SAM junctions at -0.5 V under different conditions. (A-C) K-1 under protonated conditions. (D-F) K-1 under deprotonated conditions. The red curves represent the Gaussian fits to these histograms. All J-V measurements were performed at room temperature.

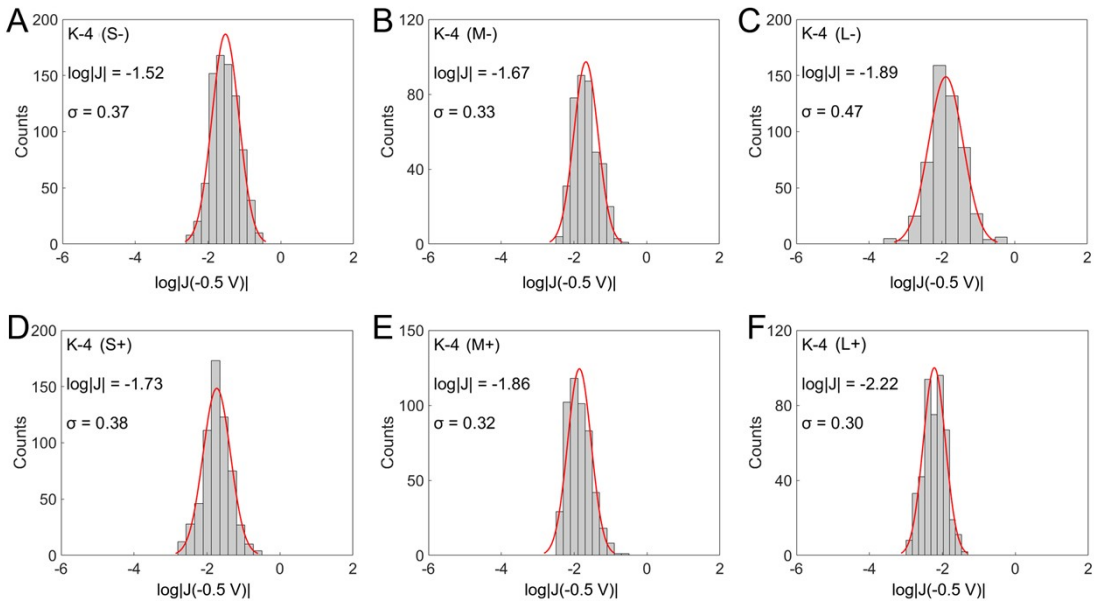

Fig. S10 log|J| distribution histograms of K-4 peptide SAM junctions at -0.5 V under different conditions. (A-C) K-4 under protonated conditions. (D-F) K-4 under deprotonated conditions. The red curves represent the Gaussian fits to these histograms. All J-V measurements were performed at room temperature.

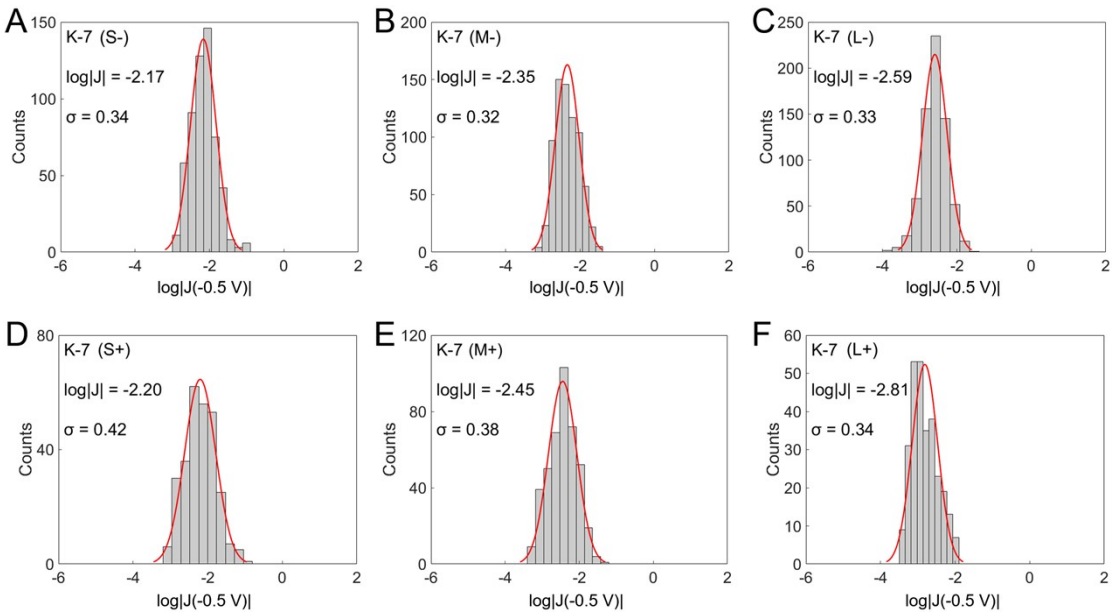

Fig. S11 log|J| distribution histograms of K-7 peptide SAM junctions at -0.5 V under different conditions. (A-C) K-7 under protonated conditions. (D-F) K-7 under deprotonated conditions. The red curves represent the Gaussian fits to these histograms. All J-V measurements were performed at room temperature.

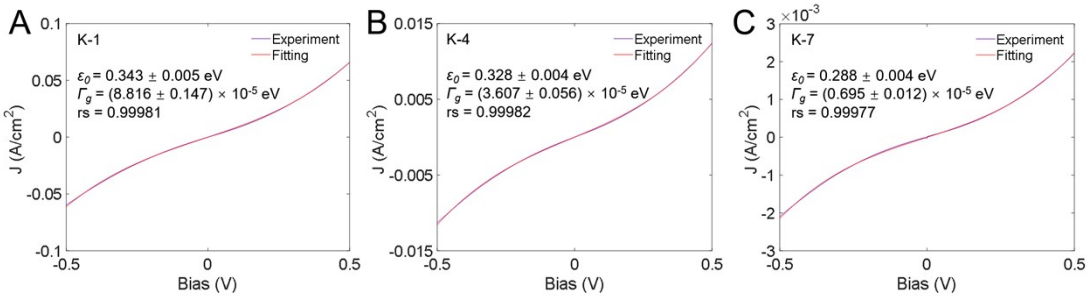

Fig. S12 Comparison of the experimental J-V curves and fitting results for peptide SAM junctions: (A) K-1. (B) K-4. (C) K-7. Experimental data are in blue and fitting results are in red. Molecules-electrodes energy barrier height (ε_0), the energy level broadening (Γ_g), and the quality of the fittings (rs) are extracted from the peptide J-V curves fitting by Landauer formula.

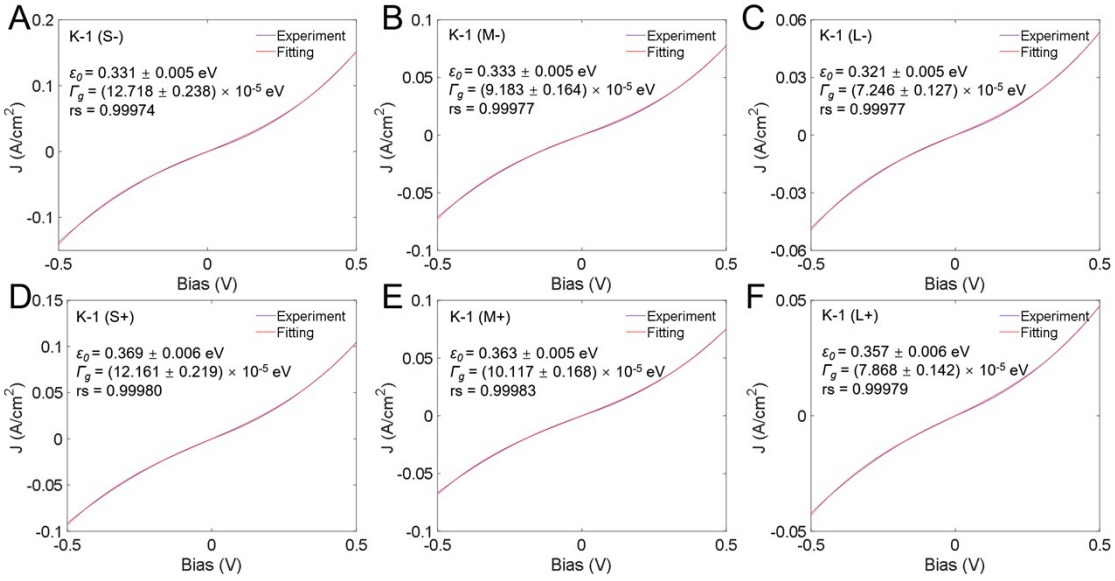

Fig. S13 Comparison of the experimental J-V curves and fitting results for peptide SAM junctions: (A-C) K-1 under protonated conditions. (D-F) K-1 under deprotonated conditions. Experimental data are in blue and fitting results are in red. Molecules-electrodes energy barrier height (ε_0), the energy level broadening (Γ_g), and the quality of the fittings (rs) are extracted from the peptide J-V curves fitting by Landauer formula.

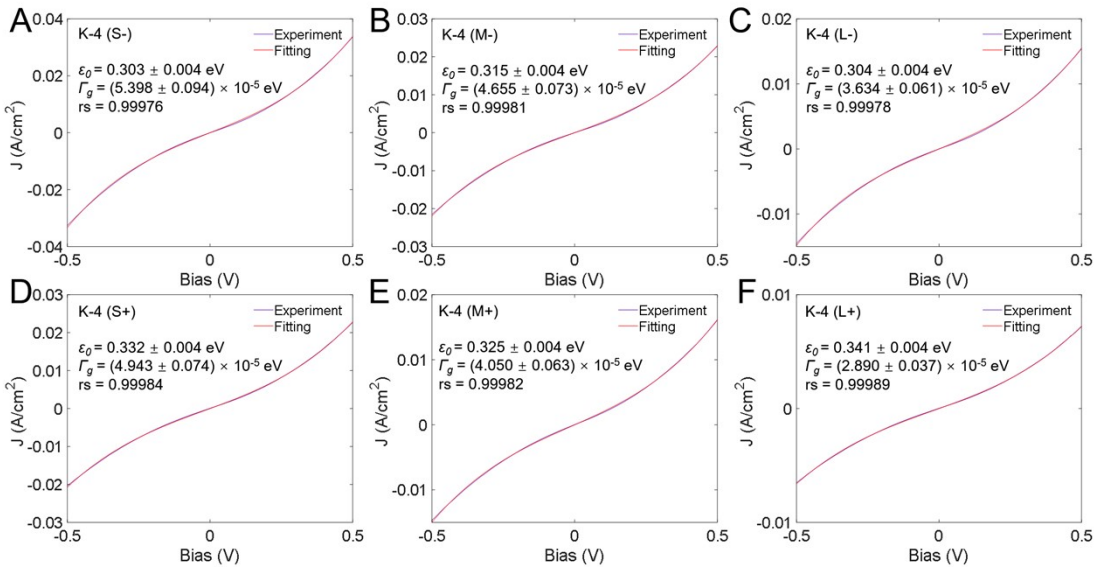

Fig. S14 Comparison of the experimental J-V curves and fitting results for peptide SAM junctions: (A-C) K-4 under protonated conditions. (D-F) K-4 under deprotonated conditions. Experimental data are in blue and fitting results are in red. Molecules-electrodes energy barrier height (ε_0), the energy level broadening (Γ_g), and the quality of the fittings (rs) are extracted from the peptide J-V curves fitting by Landauer formula.

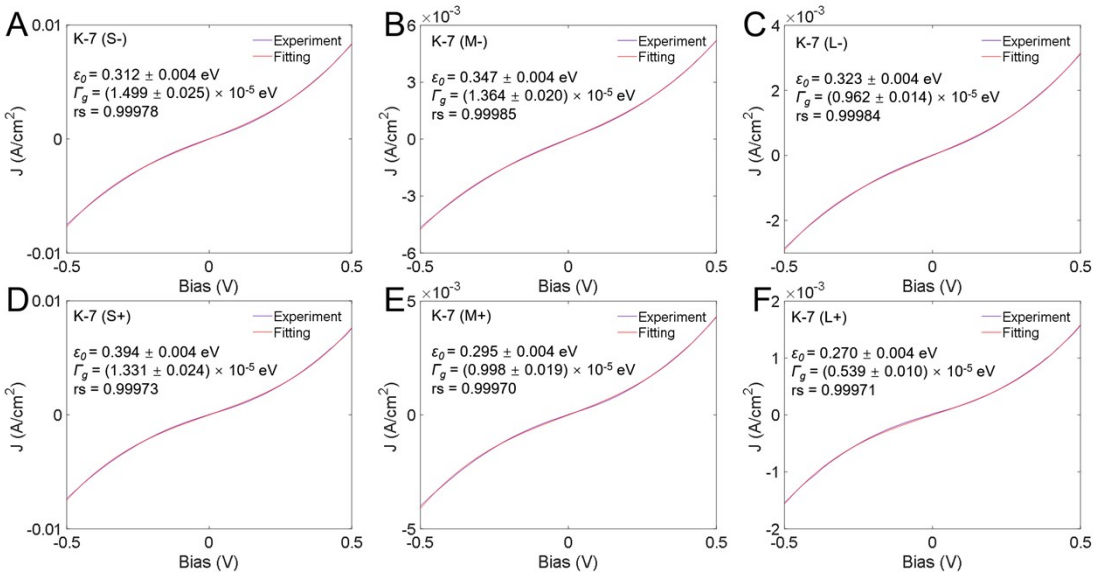

Fig. S15 Comparison of the experimental J-V curves and fitting results for peptide SAM junctions: (A-C) K-7 under protonated conditions. (D-F) K-7 under deprotonated conditions. Experimental data are in blue and fitting results are in red. Molecules-electrodes energy barrier height (ε_0), the energy level broadening (Γ_g), and the quality of the fittings (rs) are extracted from the peptide J-V curves fitting by Landauer formula.

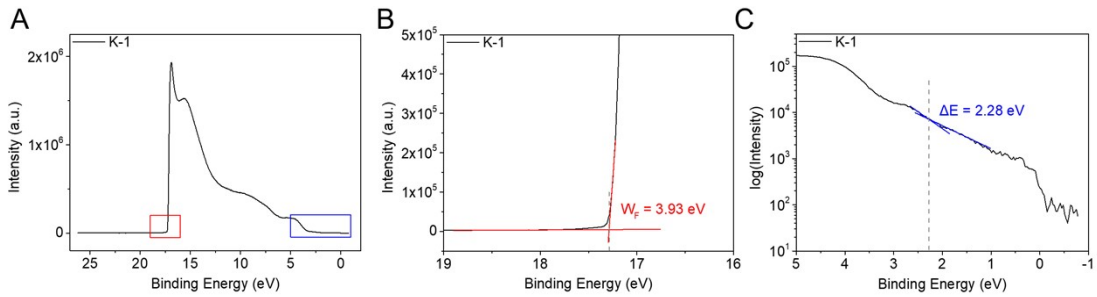

Fig. S16 Obtained W_F and ΔE from UPS spectra. (A) Typical UPS spectrum of K-1 SAM on the Au substrate. (B) The region of photoemission cutoff (marked by red rectangle in panel A). (C) The region of photoemission onset (marked by blue rectangle in panel A).

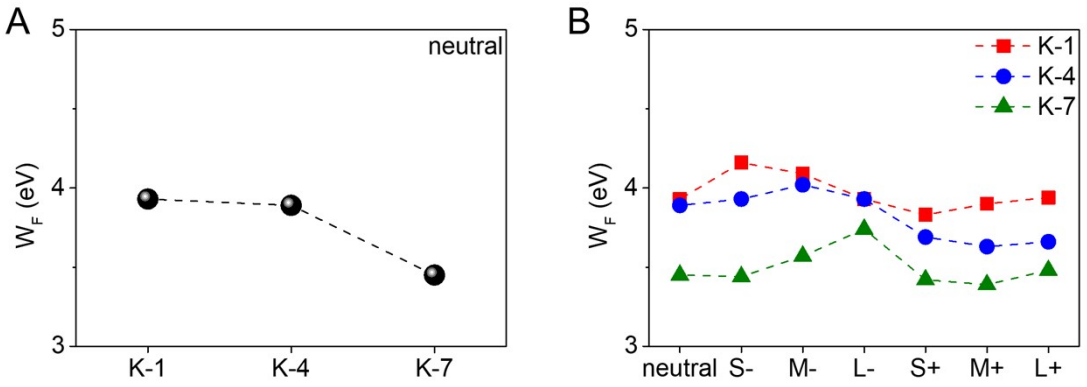

Fig. S17 The work function (W_F) of peptide SAMs from UPS measurement. (A) W_F varies with the lysine-doped position under neutral condition. (B) W_F varies with the counterions under different conditions.

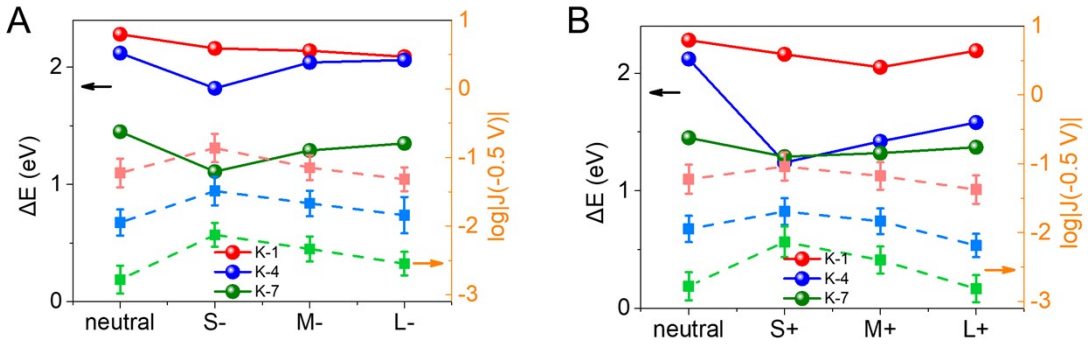

Fig. S18 The Fermi-HOMO energy offset obtained from UPS (ΔE) and log|J| at -0.5 V varies with counterion size. (A) Peptide SAMs under protonated conditions. (B) Peptide SAMs under deprotonated conditions. The solid and dashed lines represent ΔE and log|J| at -0.5 V, respectively.

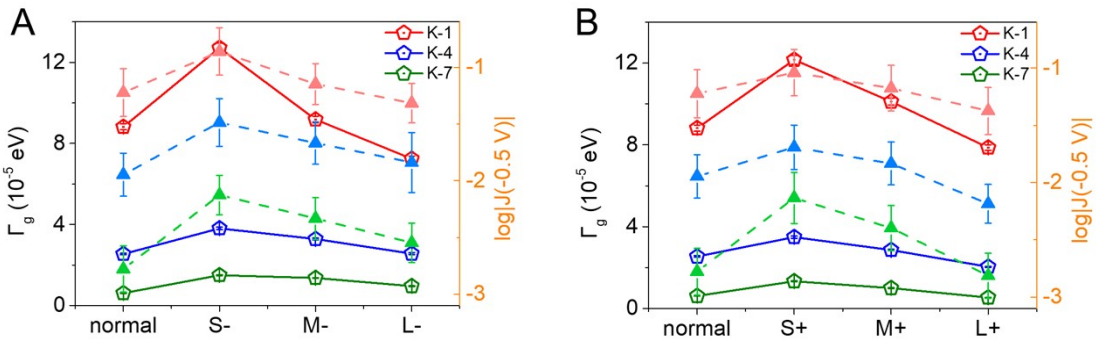

Fig. S19 Trend plots of Γ_g and log|J| at -0.5 V for peptide SAMs. (A) Peptide SAMs under protonated conditions. (B) Peptide SAMs under deprotonated conditions. The solid and dashed lines represent Γ_g and log|J| at -0.5 V, respectively.

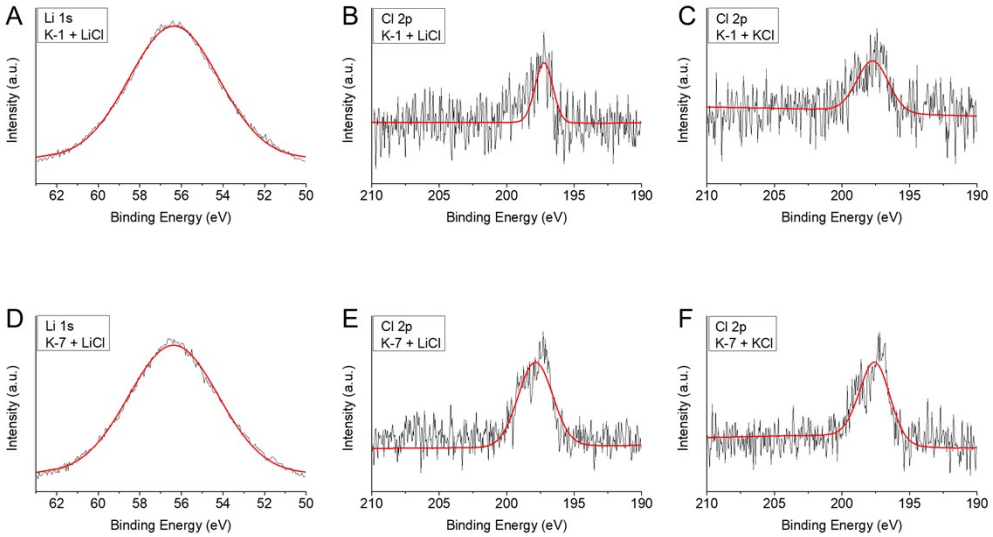

Fig. 20 XPS spectra of K-1 and K-7 SAMs on the Au substrate. XPS spectra of (A) Li *1s* after LiCl treatment, (B) Cl *2p* after LiCl treatment, and (C) Cl *2p* after KCl treatment in K-1 SAMs. XPS spectra of (D) Li *1s* after LiCl treatment, (E) Cl *2p* after LiCl treatment, and (F) Cl *2p* after KCl treatment in K-7 SAMs.

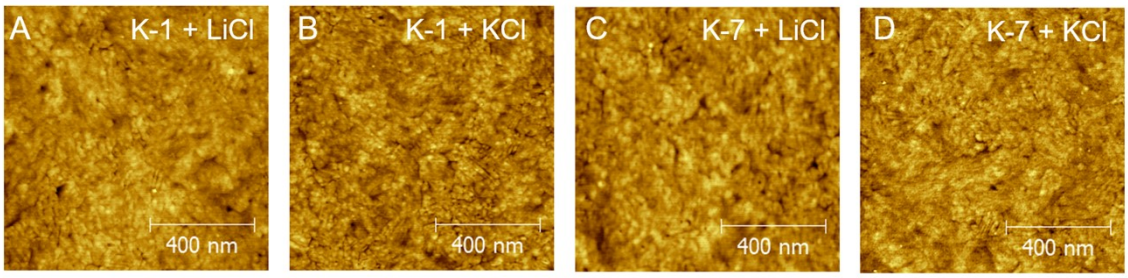

Fig. 21 Surface topographies of peptide SAMs measured by AFM images. (A-B) K-1 SAM treated with LiCl and KCl, respectively. (C-D) K-7 SAM treated with LiCl and KCl, respectively.

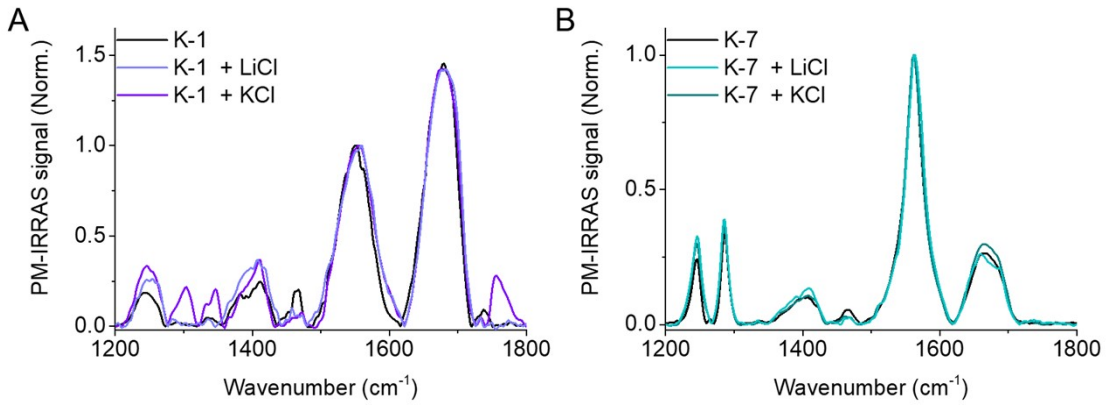

Fig. 22 Normalized PM-IRRAS spectra of the peptide SAMs with 4 cm^{-1} band resolution in the range of 1200-1800 cm^{-1}. (A) K-1 SAM treated with LiCl and KCl. (B) K-7 SAM treated with LiCl and KCl. The black curves show the PM-IRRAS spectra under neutral condition in all panels for comparison.

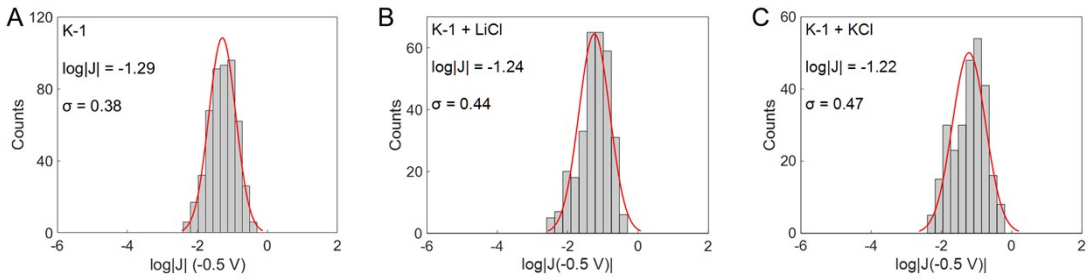

Fig. 23 log|J| distribution histograms of K-1 SAM junctions at -0.5 V under different conditions. (A) K-1 SAM under neutral condition. (B) K-1 SAM treated with LiCl. (C) K-1 SAM treated with KCl. The red curves represent the Gaussian fits to these histograms.

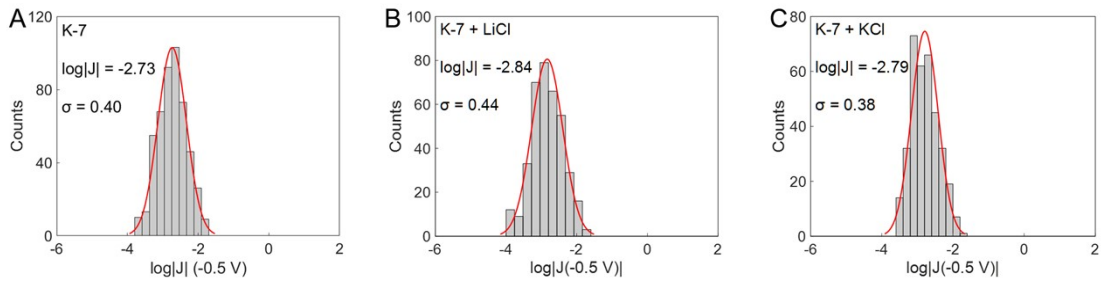

Fig. 24 log|J| distribution histograms of K-7 SAM junctions at -0.5 V under different conditions. (A) K-7 SAM under neutral condition. (B) K-7 SAM treated with LiCl. (C) K-7 peptide SAM treated with KCl. The red curves represent the Gaussian fits to these histograms.

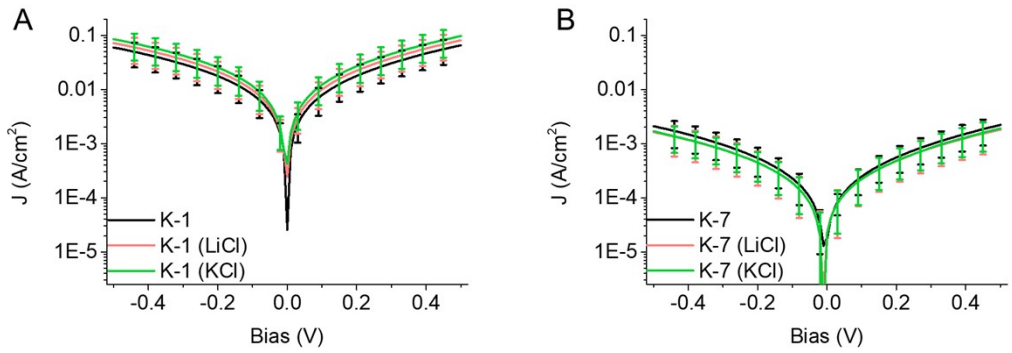

Fig. 25 Semilog plots of J-V for K-1 and K-7 peptide junctions under different conditions. (A) K-1 SAM treated with LiCl and KCl. (B) K-7 SAM treated with LiCl and KCl. The black curves show the J-V plots under neutral condition in all panels for comparison.

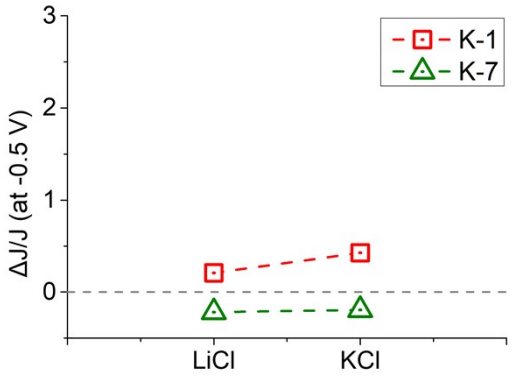

Fig. 26 Plots of ΔJ/J at -0.5 V for K-1 and K-7 peptide SAMs treated with LiCl and KCl. ΔJ/J = (J' - J)/J, J' is the current density under different conditions and J is the current density under neutral condition at -0.5 V. Gray dotted line at y = 0 is guide to the eyes, standing for the current density under neutral condition.

Table S1 Thickness of peptide SAMs under different conditions determined by ellipsometry.

	Thickness (Å)		
	K-1	K-4	K-7
neutral	15.2 ± 0.4	22.5 ± 1.5	28.2 ± 0.5
S-	16.1 ± 0.4	23.0 ± 1.3	28.7 ± 0.5
M-	17.0 ± 0.7	22.7 ± 0.6	29.0 ± 0.4
L-	17.5 ± 0.9	23.1 ± 0.7	29.1 ± 0.7
S+	15.9 ± 0.6	21.4 ± 1.2	28.6 ± 0.6
M+	15.9 ± 1.0	21.5 ± 0.8	29.1 ± 1.0
L+	16.9 ± 0.8	22.5 ± 1.1	29.0 ± 0.3

Table S2 Absorbance of amide I and II, and their ratios for K-1, K-4, and K-7 peptide SAMs under different conditions.

	Amide I (cm^{-1})	Amide II (cm^{-1})	Amide I/II ratio
K-1	1680	1550	1.46
K-1 (S-)	1680	1552	1.51
K-1 (M-)	1680	1550	1.33
K-1 (L-)	1680	1552	1.67
K-1 (S+)	1678	1552	1.73
K-1 (M+)	1678	1554	1.52
K-1 (L+)	1678	1554	1.60
K-4	1672	1556	0.64
K-4 (S-)	1678	1556	0.67
K-4 (M-)	1678	1554	0.83
K-4 (L-)	1678	1562	0.49
K-4 (S+)	1678	1556	0.76
K-4 (M+)	1680	1554	0.82
K-4 (L+)	1678	1554	0.70
K-7	1665	1562	0.26
K-7 (S-)	1664	1562	0.28
K-7 (M-)	1672	1562	0.23
K-7 (L-)	1666	1562	0.24
K-7 (S+)	1674	1562	0.36
K-7 (M+)	1662	1562	0.23
K-7 (L+)	1678	1562	0.27

Table S3 Thickness of peptide SAMs treated with LiCl and KCl determined by ellipsometry.

	Thickness (Å)	
	K-1	K-7
neutral	15.2 ± 0.4	28.2 ± 0.5
LiCl	15.5 ± 0.3	27.3 ± 0.5
KCl	15.6 ± 0.6	28.0 ± 1.5

Table S4 Absorbance of amide I and II, and their ratios for K-1 and K-7 peptide SAMs treated with LiCl and KCl.

	Amide I (cm^{-1})	Amide II (cm^{-1})	Amide I/II ratio
K-1	1680	1550	1.46
K-1 (LiCl)	1678	1556	1.42
K-1 (KCl)	1683	1560	1.42
K-7	1665	1562	0.26
K-7 (LiCl)	1660	1564	0.26
K-7 (KCl)	1664	1562	0.30

References

[1] Hegner, M.; Wagner, P.; Semenza, G., Ultralarge atomically flat template-stripped Au surfaces for scanning probe microscopy. *Surf. Sci.* **1993,** *291*, 39-46.

[2] Weiss, E. A.; Kaufman, G. K.; Kriebel, J. K.; Li, Z.; Schalek, R.; Whitesides, G. M., Si/SiO_2-templated formation of ultraflat metal surfaces on glass, polymer, and solder supports: their use as substrates for self-assembled monolayers. *Langmuir* **2007,** *23*, 9686-9694.

[3] Mervinetsky, E.; Alshanski, I.; Lenfant, S.; Guerin, D.; Sandonas, L. M.; Dianat, A.; Gutierrez, R.; Cuniberti, G.; Hurevich, M.; Yitzchaik, S.; Vuillaume, D., Electron transport through self-assembled monolayers of tripeptides. *J. Phys. Chem. C* **2019,** *123*, 9600-9608.

[4] Arikuma, Y.; Nakayama, H.; Morita, T.; Kimura, S., Electron hopping over 100 Å along an α helix. *Angew. Chem. Int. Ed.* **2010,** *49*, 1800-1804.

[5] Rothemund, P.; Bowers, C. M.; Suo, Z. G.; Whitesides, G. M., Influence of the contact area on the current density across molecular tunneling junctions measured with EGaIn top-electrodes. *Chem. Mater.* **2018,** *30*, 129-137.

[6] Jones, T. A., Skewness and kurtosis as criteria of normality in observed frequency distributions. *J. Sediment. Res.* **1969,** *39*, 1622-1627.

[7] Chen, J.; Kim, M.; Gathiaka, S.; Cho, S. J.; Kundu, S.; Yoon, H. J.; Thuo, M. M., Understanding Keesom interactions in monolayer-based large-area tunneling junctions. *J. Phys. Chem. Lett.* **2018,** *9*, 5078-5085.

[8] Zhang, Q.; Huang, H. Z.; He, H. X.; Chen, H. F.; Shao, H. B.; Liu, Z. F., Determination of locations of sulfur, amide-nitrogen and azo-nitrogen in self-assembled monolayers of alkanethiols and azobenzenethiols on Au (111) and GaAs (100) by angle-resolved X-ray photoelectron spectroscopy. *Surf. Sci.* **1999,** *440*, 142-150.

[9] Freeman, T. L.; Evans, S. D.; Ulman, A., XPS studies of self-assembled multilayer films. *Langmuir* **1995,** *11*, 4411-4417.

[10] Lamont, C. L.; Wilkes, J., Attenuation length of electrons in self-assembled monolayers of n-alkanethiols on gold. *Langmuir* **1999,** *15*, 2037-2042.

[11] Walczak, M. M.; Popenoe, D. D.; Deinhammer, R. S.; Lamp, B. D.; Chung, C.; Porter, M. D., Reductive desorption of alkanethiolate monolayers at gold: a measure of surface coverage. *Langmuir* **1991,** *7*, 2687-2693.

[12] X. Li; P.-A. Cazadé; P. Qi; D. Thompson; C. Guo, The role of externally-modulated electrostatic interactions in amplifying charge transport across lysine-doped peptide junctions. *Chin. Chem. Lett.*, in press.

[13] Bâldea, I., Ambipolar transition voltage spectroscopy: analytical results and experimental agreement. *Phys. Rev. B* **2012,** *85*, 035442.